

# A Matlab program to invert 1D Spectral Induced Polarization data for Cole-Cole model including electromagnetic effects

Ghorbani, A.<sup>[1]</sup>, Camerlynck, C.<sup>[1]</sup>, Florsch, N.<sup>[1]</sup>

1. UMR 7619 Sisyphe, Université Pierre et Marie Curie, Paris, France.

## ABSTRACT

*An inversion code in Matlab is constructed to recover the parameters of Cole-Cole model from spectral induced polarization (SIP) data in a 1D earth. In a spectral induced polarization survey the impedances at various frequencies are recorded. Both induced polarization and electromagnetic coupling effects occur simultaneously in this frequency bandwidth, the latter being more and more dominate when frequency increases. We used CR1Dmode code published by Ingeman-Nielsen and Baumgartner (2006) as forward modelling. This code solves electromagnetic responses in the presence of complex resistivity effects in a 1D earth. A homotopy method is designed to overcome the local convergence of normal iterative methods. In addition, to further condition the inverse problem, we incorporate standard Gauss-Newton (or Quasi Newton) methods. The graphical user interfaces allow for easy data entry and the a priori model and also cable configuration. We present two synthetic examples to illustrate that the spectral parameters can be recovered from multifrequency complex resistivity data.*

## INTRODUCTION

Spectral Induced Polarization (SIP) is widely used in mineral exploration (e.g., Pelton et al., 1978, Luo and Zhang, 1998). The mutual impedances of grounded wires (electromagnetic coupling between the transmitter, the receiver and the ground) are of prime importance in SIP surveys. At low frequencies, electromagnetic (EM) couplings and normal polarization effects of the subsurface material have similar functional behaviour with respect to the conductivity of the earth and their combined effects are recorded in an SIP survey. EM coupling is a major impediment in the interpretation of induced polarization (IP) data. EM coupling also increases with the dipole length and dipole separation and with conductivity and frequency (Dey and Morrison, 1973). For deep exploration, the dipoles and their separation must be large; hence, the operational frequency is usually low to avoid EM coupling. Unfortunately, the natural EM field spectrum noise rises steeply below 1.0 Hz (Gasperiikova and Morrison, 2001). One way to avoid EM coupling is measuring SIP data at frequencies low enough that any EM coupling is either negligible or predictable. Loke et al. (2006) use a regularized least-squares optimization method to recover the SIP parameters in the 2D problem, but reduce the EM coupling phenomena by limiting the maximum frequency between 10 and 100 Hz. However, elimination of high frequency IP spectrum, eliminates the important information.

A forward modelling code has been developed that is capable of handling several commonly used electrical and electromagnetic methods in a 1D environment by Ingeman-Nielsen and Baumgartner (2006). This code calculates the mutual impedance in different frequencies of 1D ground layers for Cole-Cole model and different grounded electrode arrays. Also, it considers the influence caused by the placement of the wires.

Homotopy method is a powerful tool for solving nonlinear problems due to its widely convergent properties (Watson, 1989). Homotopy is widely used in geophysical methods to solve the non linear problems (e.g., Vasco, 1998; Jegen et al., 2001; Bao and Liu, 2003; Han et al., 2007).

This poster discusses the development of the homotopy inversion in 1D for IP and EM coupling integral according to forward modelling code (CR1Dmod) of Ingeman-Nielsen and Baumgartner (2006). At first, inversion process is reviewed and then, program structure is discussed. At last, the results of inversion code for the synthetic data are presented.

## INVERSION PROCESS

In this section we explain the continuation (homotopy) inversion process. The input data consist of amplitude and phase at a number of frequencies that are converted to real and imaginary resistivity values during the inversion processes. The

measurements should be performed for at least four frequencies spread over a suitably wide range since a single simple Cole-Cole model has four parameters. The parameter vector  $\mathbf{P}$  finally reduces to:

$$\left[ \hat{\rho}_{0i}, \hat{m}_i, \hat{c}_i, \hat{\tau}_i, \hat{h}_i \right]^T$$

where

$$\begin{aligned} \hat{\rho}_{0i} &= \log(\rho_{0i}) \\ \hat{m}_i &= \log\left(\frac{m_i}{1-m_i}\right) \\ \hat{c}_i &= \log\left(\frac{c_i}{1-c_i}\right) \\ \hat{h}_i &= \log(h_i) \end{aligned}$$

and  $i$  is layer index. The change affecting Cole-Cole parameters are explained in details by Ghorbani et al., 2007. The first part is the determination of a 1D initial resistivity model from the DC apparent resistivity values by an approximate inversion. The amplitudes of the apparent-impedance values that are measured at the lowest frequency can be used as the DC resistivity values. To invert the  $\hat{\rho}_{0i}$  and  $\hat{h}_i$  in initial model,  $m_i$  is considered zero. Therefore in this case, forward modelling is similar to DC resistivity model. The second part consist the homotopy method that use Gauss-Newton or Quasi-Newton methods to minimization of misfit function in each step. The parameters obtained in the earlier part are used to compute the starting

model of the homotopy inversion. We use a linear combination function of  $g(\mathbf{P})$  (Jegen et al., 2001):

$$\mathbf{h}(\mathbf{P}, \lambda) = \lambda \mathbf{d}_{obs} + (1-\lambda) \mathbf{g}_0(\mathbf{P}_0) \quad (1)$$

Where  $\mathbf{d}_{obs}$  is the vector of in-phase and out-of-phase parts of complex resistivity measurements;  $\mathbf{g}_0$  is the vector of real and imaginary resistivity obtained from forward modelling by starting parameter vector  $\mathbf{P}_0$ ;  $\mathbf{P}$  is the parameter vector and  $\lambda$  is a real variable that changes between 0 and 1. Here, it is assumed that the physics-based forward response capable of predicting the data vector,  $\mathbf{d}=\mathbf{g}(\mathbf{P}^*)$ . The first value of  $\lambda$  is 0 and increases in later steps. It is clear that  $\mathbf{g}(\mathbf{P}, \lambda=0) = \mathbf{g}_0(\mathbf{P}_0)$  is the same starting model vector. When  $\lambda$  increases, the other model vectors are estimated so the effect of data measurements vector increases and the effect of the initial model vector decreases. In this work, path tracking is based on a set of predictor-corrector steps. The predictor step consists of varying the model vector ( $\mathbf{P}, \lambda$ ) by  $\Delta\lambda$  along the  $\lambda$ -direction (Benavides and Everett, 2006). We used an isometric division for  $\Delta\lambda$  or  $\lambda_j = j/N$  where  $j = 1, \dots, N$  as it proves to give satisfactory results (Benavides and Everett, 2006; Han et al., 2007). The corrector step is a Gauss-Newton (or Quasi-Newton) algorithm that is used for minimization of the misfit function in each step of homotopy inversion. Once the corrector step is terminated, the next predictor step is initiated. At the  $j^{\text{th}}$  predictor-corrector step, the predicted model vector is  $(\mathbf{P}_{k,j}\Delta\lambda)$ . Assuming that the solution  $\mathbf{P}^j$  of the  $j^{\text{th}}$  equation has already been obtained, the successive Gauss-Newton (or Quasi-Newton) method can be used to solve the  $(j+1)^{\text{th}}$  equation. Then the iteration formula for solve  $j^{\text{th}}$  step of homotopy equation 1 with considering Gauss-Newton (e.g., Mosegaard and Tarantola, 2002) is following:

$$\mathbf{P}_{k+1}^j = \mathbf{P}_k^j - \varepsilon_k \left( \mathbf{G}_k^T \mathbf{C}_{\mathbf{d}_0 \mathbf{d}_0}^{-1} \mathbf{G}_k + \mathbf{C}_{\mathbf{p}_0 \mathbf{p}_0}^{-1} \right)^{-1} \times \left[ \mathbf{G}_k^T \mathbf{C}_{\mathbf{d}_0 \mathbf{d}_0}^{-1} \left( \mathbf{g}(\mathbf{P}_k) - \mathbf{h}(\mathbf{P}_k, \lambda_j) \right) + \mathbf{C}_{\mathbf{p}_0 \mathbf{p}_0}^{-1} \left( \mathbf{P}_k - \mathbf{P}_{prior} \right) \right] \quad (2)$$

where  $k$  is iteration index of the Gauss-Newton iterations and  $k = 0, 1, \dots, k_r$   
or

$$\mathbf{P}_{k+1}^j = \mathbf{P}_k^j - \varepsilon_k \left( \mathbf{G}_k^T \mathbf{C}_{\mathbf{d}_0 \mathbf{d}_0}^{-1} \mathbf{G}_k + \mathbf{C}_{\mathbf{p}_0 \mathbf{p}_0}^{-1} \right)^{-1} \times \left\{ \mathbf{G}_k^T \mathbf{C}_{\mathbf{d}_0 \mathbf{d}_0}^{-1} \left[ \mathbf{g}(\mathbf{P}_k) - \left( \left( 1 - \frac{j}{N} \right) \mathbf{g}_0(\mathbf{P}_0) + \frac{j}{N} \mathbf{d}_{obs} \right) \right] + \mathbf{C}_{\mathbf{p}_0 \mathbf{p}_0}^{-1} \left( \mathbf{P}_k - \mathbf{P}_{prior} \right) \right\} \quad (3)$$

The Jacobian-matrix values are obtained from numerical derivative of forward modelling. The calculation of the Jacobian matrix can be the most time-consuming step of the inversion process. In order to reduce the computing time, Loke and Dahlin (2002) used a quasi-Newton method to estimate the Jacobian matrix values. We used both of the methods in inversion algorithm.

### PROGRAM STRUCTURE

CR1Dinv consists of three main windows: *CR1Dinv* window, *SondagePoint* window and *Calculate* window. *CR1Dinv* window controls the starting parameters and its standard deviation and number of sounding data; *SondagePoint* window controls the configuration of the sounding points; *Calculate*

window controls the calculation specific parameters and inversion routines. The left-hand side of *CR1Dinv* window features an interactive plot of the half-space model (Figure 1). By mouse clicking into the plot, the user can insert layer boundaries and drag them to the desired position. In the right-hand side of the same window, the lower section gives input fields for the a priori layer parameters, including a priori Cole-Cole model parameters and its standard deviation, relative permittivity ( $\varepsilon_r = \varepsilon / \varepsilon_0$ ) and magnetic susceptibility ( $X = \mu / \mu_0 - 1$ ), it also allows for adding and deleting layers in the model. The upper right hand section of this window gives control of the measurement configurations. Dipole-Dipole array and general surface array (GSA) are accessible. GSA allows for arbitrary location of receiver and transmitter electrodes on the surface of the layered half-space.

*SondagePoint* window (Figure 2) has appeared and allows the user to enter the position of electrodes. There is a column of *topview* buttons on left hand of *SondagePoint* window. By left and then right clicking the mouse on the *topview* buttons, a special window is called that allows the user to place the electrodes, either by dragging them with the mouse, or by entering new coordinates in the input fields, in left part of one. In the right hand of this window is an Excel spread sheet that let the user enters the data spectrum (frequency in Hertz, amplitude in ohm meter, negative phase in milliradian, Amplitude error in percent and phase error in milliradian). In *Calculate* window (Figure 3), parameters specific to the type of calculation can be adjusted before calling the forward modelling routine (Ingeman-Nielsen and Baumgartner, 2006) and also specific inversion routines. Forward modelling and inversion routines are in *emgsafwd.m* and *Inversion.m* files respectively.

Different parameters that are used in the inversion part of *Calculate* window include: The homotopy coefficient determines the maximum division number along  $\lambda$ -direction.  $\lambda$  is the homotopy parameter that varies between 0 and 1. The improvement in the RMS error is considered as criterion for termination at each homotopy inversion step. Gauss-Newton and Quasi-Newton options allow using for minimization of the misfit function in each step of homotopy inversion and iteration adjustment is the same  $\epsilon$  ad-hoc (real, positive) value that is explained in formula 2 and 3. After the calculations have ended, results are saved into a binary Matlab file along with the model, configuration and inverted parameters. Finally, calculated responses are plotted as Argand diagrams onto the screen. For each layer plots present convergence processes for each of parameter.

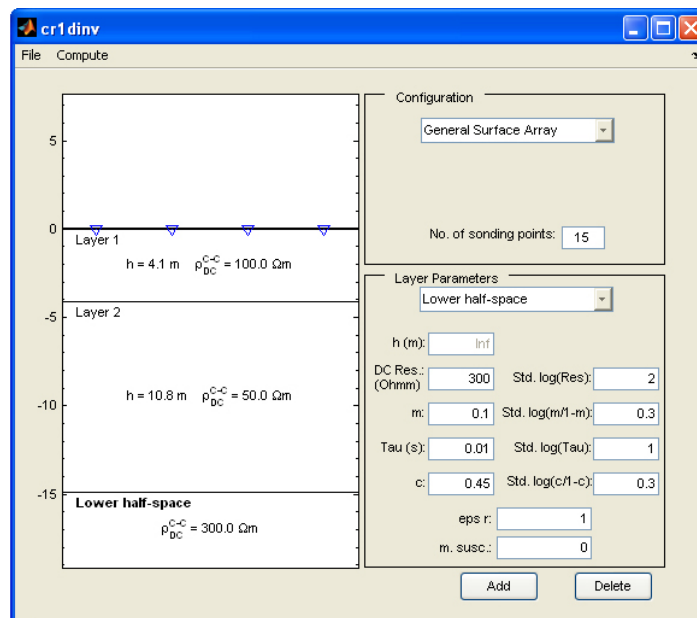


**Figure 1:** *CR1Div* window: a graphical representation of the model, in which the user can add or delete layers and move boundaries. Right-hand side of the window gives control of the configuration, a priori layer parameters and a priori layer parameters standard deviation of the model.

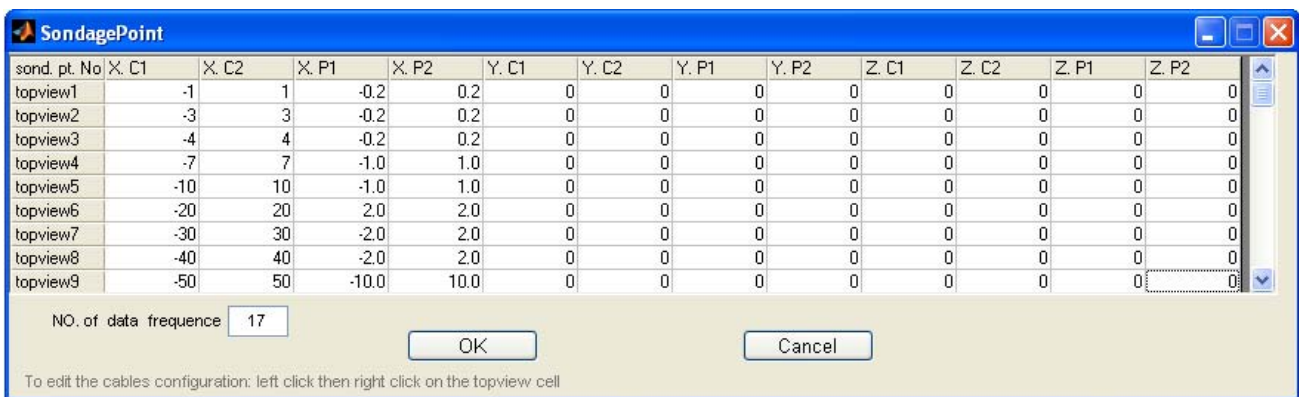


**Figure 2:** Sounding point window of *CR1Div* features a spread sheet that allows entering the electrodes coordinate. Left and then right Click the mouse gives access to *topview* windows as edit the cable configuration of each sounding point.

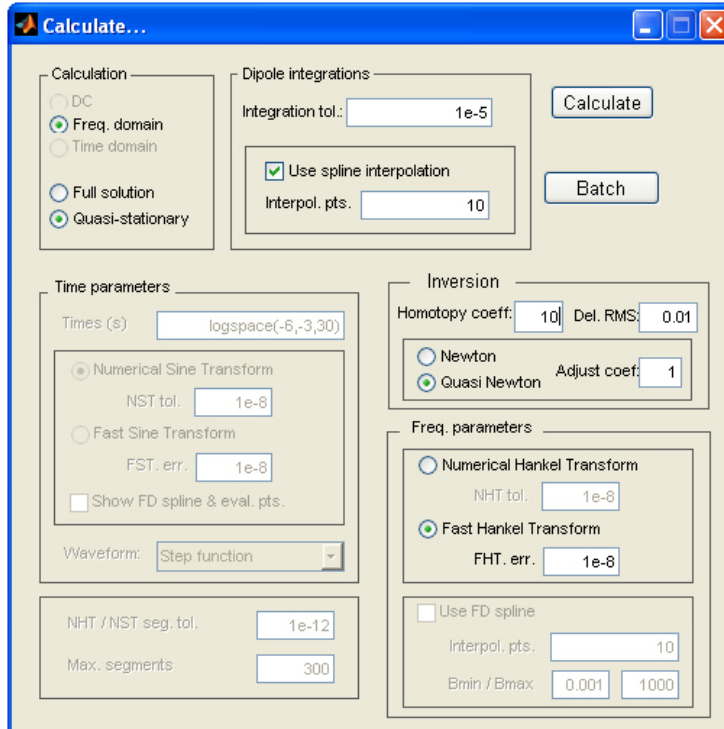


Figure 3: Calculate window of CR1Dinv gives user control over calculation domain, transform types, tolerances and spline interpolations.

Table 1: Inversed parameters are obtained during inversion algorithm for synthetic spectral induced polarization data. Earth is proposed half-space. Real values of parameters are presented.

	Layers	$\rho_0(\Omega m)$	m	c	$\tau(s)$	$std(\hat{\rho}_0)$	$std(\hat{m})$	$std(\hat{c})$	$std(\hat{\tau})$	RMS error (%)
Real values	1	50	0.8	0.3	0.1	1	0.5	0.5	1	0.3
Inversion		49.98	0.7998	0.30	0.0998					

Table 2: Inversed parameters are obtained during inversion algorithm for synthetic spectral induced polarization data. Earth is proposed containing two layers. Real values of parameters are presented.

	Layers	$\rho_0(\Omega m)$	m	c	$\tau(s)$	h(m)	$std(\hat{\rho}_0)$	$std(\hat{m})$	$std(\hat{c})$	$std(\hat{\tau})$	$std(\hat{h})$	RMS error (%)
Real values	1	50	0.3	0.3	1	5	1	0.5	0.5	1	0.1	2.6
Inversion		49.9	0.30	0.30	0.97	4.96						
Real values	2	300	0.05	0.8	0.01	-	1	0.5	0.5	1	-	
Inversion		299.7	0.05	0.77	0.01	-						

### RESULTS

The results from two synthetic examples with the inversion method are presented. Minimum version is a Matlab environment version 7.0.4 (R14). We used 17 frequencies in the 0.183 Hz to 12 kHz range. The first example model consists of a half-space earth. Table 1 shows the real and inversion values of parameters. The amplitude and phase values are calculated for 5 sounding points, obtained from a Dipole-Dipole array. The distance array line AB=MN=50 m and n, Dipole-Dipole separation, changes from 1 to 5. Transmitter and receiver cables are in same line. The recovered parameters agree well with the

true values. The number of parts in  $\lambda$ -direction is 10 ( $\Delta\lambda = 0.1$ ). Root mean square error (RMS) is obtained 0.3%.

The second test model consists in a two horizontal layers mode with thickness of upper layer 5 m. Table 2 shows the model and inverted parameters. The amplitude and phase values are calculated for 5 sounding points, obtained from Schlumberger array. The transmitter lines AB change from 0.6 to 60 meter. Transmitter and receiver cables are in same line. The other conditions that are assumed in inversion process include; the homotopy inversion consist of 5 steps and the Quasi-Newton is considered for misfit minimization. Table 2 shows the recovered electrical parameters agree well with the true values.

## CONCLUSION

A homotopy inversion method for SIP data using the Cole-Cole model is proposed based on electromagnetic formulation of a 1D earth. This method further widens the domain of convergence of traditional methods. In this work, path tracing is based on a set of predictor-corrector steps. Local inversion methods of Gauss-Newton and/or quasi Newton are used as corrector step. An approximate inversion of the DC resistivity model is first carried out to construct the initial resistivity and thickness models, and this is then used as the starting model in the final inversion. We modified CR1Dmod and designed CR1Dinv code for SIP inversion process. It has given satisfactory results in tests with data from synthetic models.

## ACKNOWLEDGEMENTS

We are indebted to the ANR-CNRS-INSU-ECCO program (project Polaris II, 2005-2007) in France for supporting the completion of this work.

## REFERENCES

- Bao, G. and Liu, J., 2003, Numerical solution of inverse scattering problems with multi-experimental limited aperture. *SIAM Journal on Scientific Computing*, 25, 1102–1117.
- Benavides, A., Everett, M. E., 2006, Non-linear inversion of controlled source multi-receiver electromagnetic induction data for unexploded ordnance using a continuation method, *Journal of Applied Geophysics*, in press.
- Dey, A. and Morrison, H.F., 1973, EM coupling in frequency and time-domain induced-polarization surveys over a multilayered Earth, *Geophysics*, 38, no. 2, 380–405.
- Ghorbani, A., Camerlynck, C., Florsch, N., Cosenza, P. and Revil, A., 2007, Bayesian Inference of the Cole-Cole Parameters from Time and Frequency Domain Induced Polarization, *Geophysical Prospecting*, in press 2007.
- Han, B., Fu, H. and Liu, H., 2007, A homotopy method for well-log constraint waveform inversion, *Geophysics*, 72, no. 1, R1–R7.
- Gasparikova, E. and Morrison, H.F., 2001, Mapping of induced polarization using natural fields, *Geophysics* 66, 137–147.
- Ingeman-Nielsen, T. and Baumgartner, F., 2006, CR1Dmod: A Matlab program to model 1D complex resistivity effects in electrical and EM surveys, *Computers and Geosciences*, 32, 1411–1419.
- Jegen, M.D., Everett, M.E. and Schultz, A., 2001, Using homotopy to invert geophysical data. *Geophysics*, 66, 1749–1760.
- Loke, M.H., Chambers, J.E. and Ogilvy, R.D., 2006, Inversion of 2D spectral induced polarization imaging data, *Geophysical Prospecting*, 54, 287–301.
- Loke, M.H. and Dahlin, T., 2002, A comparison of the Gauss–Newton and quasi-Newton methods in resistivity imaging inversion, *Journal of Applied Geophysics*, 49, 149–162.
- Luo, Y., and Zhang, G., 1998, Theory and Application of Spectral Induced Polarization, *Geophysical Monograph Series*.
- Mosegaard, K., and Tarantola, A., 2002, Probabilistic Approach to Inverse Problems: *International Handbook of Earthquake and Engineering Seismology (Part A)*, Academic Press, 2002, pages 237–265.
- Pelton, S.H., Ward, S.H., Hallof, P.G., Sill, W.R. and Nelson, P.H., 1978, Mineral discrimination and removal of inductive coupling with multifrequency IP. *Geophysics* 43, 588–609.
- Vasco, D.W., 1998, Regularization and trade-off associated with nonlinear geophysical inverse problems: penalty homotopies: *Inverse Problems*, 14, 1033–1052.
- Watson, L. T., 1989, Globally convergent homotopy methods: A tutorial: *Applied Mathematics and Computation*, 31, 369–396.